Intrastrand Cross-Linked Actin between Gln-41 and Cys-374. II. Properties of Cross-Linked Oligomers†

Eldar Kim,‡ Martin Phillips,‡ György Hegyi,§ Andras Muhlrad,‡,|| and Emil Reisler*,‡

Department of Chemistry and Biochemistry and the Molecular Biology Institute, UCLA, Los Angeles, California 90095, and Department of Biochemistry, Eötvös Lorand University, H-1088 Budapest, Hungary

Received May 29, 1998; Revised Manuscript Received September 24, 1998

ABSTRACT: Actin filaments partially cross-linked with ANP (*N*-(4-azido-2-nitrophenyl)-putrescine between Gln-41 and Cys-374 on adjacent monomers in the long-pitch helix were depolymerized and fractionated into pools of longitudinal cross-linked dimers ($s°_{20,w} = 5.55 \pm 0.22$ S), trimers ($s°_{20,w} = 6.93 \pm 0.12$ S), and higher-order oligomers. Competition binding experiments of myosin subfragment (S1) to cross-linked dimers in the presence of pyrenyl G-actin revealed about 2 orders of magnitude stronger binding of the first than that of the second S1 molecule to actin dimer. Under similar conditions the unpolymerized cross-linked actin species activated the MgATPase of S1 only severalfold compared to 70-fold activation by F-actin. The cross-linked dimers, trimers, and oligomers were polymerized into filaments by $MgCl_2$ faster than un-cross-linked actin. In electron micrographs these filaments appeared sometimes shorter and had greater tendency to bend than un-cross-linked actin filaments. Small amounts of cross-linked actin dimers nucleated S1-induced polymerization of actin, but the polymerization by S1 was inhibited for pure populations of cross-linked dimers, trimers, and oligomers. The cross-linked dimers did not decrease the kinetic difference between the polymerization of actin by S1 isozymes S1(A1) and S1(A2). According to electron microscopy evidence, cross-linked actin oligomers polymerized by S1 yielded much shorter arrowhead structures than the un-cross-linked actin. These results indicate the importance of lateral actin−actin interaction for the activation of myosin ATPase and the polymerization of actin by S1.

The results of several investigations published in the recent years sharpened the interest in the modes of attachment of myosin heads to F-actin[1] during the cross-bridge cycle. The possibility that S1 cycles between states in which it is bound to one or two actin monomers in F-actin appears attractive in view of evidence supporting the binding of S1 to two actins. This evidence includes the structures obtained by docking atomic structure of S1 onto a model of the F-actin (*1*−*3*), the cross-linking of S1 to two actin monomers in the filament (*4*−*6*), and kinetic considerations of S1 binding to G-actin (*7*−*9*). In all of these studies the S1 is proposed to bind to two adjacent actins along the long-pitch helix. The characterization of such $(actin)_2$−S1 complexes on F-actin, except for proteolytic and cross-linking approaches, is complicated by their equilibration with the equimolar actin-S1 states.

The studies of G-actin polymerization by S1 have led Carlier and her collaborators to postulate that this process involves the formation and assembly of S1 complexes with one (GS1) and two (G_2S1) actin monomers (*7*−*11*). It has been proposed by these authors that the S1 intermediate of G-actin assembly by S1, G_2S1, corresponds to the longitudinal $(actin)_2$−S1 complex in F-actin (*12*) and that the G_2S1 structure is a good model of F-actin-S1 interface. However, the properties of G_2S1 could not be evaluated in any depth because of their transient nature.

Although the conclusions of the Carlier group about the significant presence off G_2S1 in G-actin mixtures with S1 were contested (*13*, *14*), the intrastrand cross-linking of F-actin by ANP (4-azido-2-nitrophenyl-putrescine) (*15*) provided the impetus for the isolation in this work of ANP cross-linked actin dimers, trimers, and higher-order oligomers. These materials were needed in the next part of this study for the preparation of uniformly cross-linked actin filaments and the evaluation of their mechanical properties in the in vitro motility experiments (*16*). Importantly, also, the cross-linked longitudinal dimers and oligomers provide materials unavailable until now for assessing S1 binding and S1 ATPase activity with such organized actin structures. The results of such experiments are described in this study.

MATERIALS AND METHODS

Reagents. Distilled and Millipore-filtered water and analytical grade reagents were used in all experiments. ATP, β-mercaptoethanol, and Sephadex G-150 were purchased from Sigma Chemical Co. (St. Louis, MO). *N*-(1-Pyrenyl)-iodoacetamide was obtained from Molecular Probes (Eugene,

|| Permanent address: Department of Oral Biology, Hebrew University Hadassah School of Dental Medicine, Jerusalem 91120, Israel.

† This work was supported by grants from Hungarian National Research Fund OTKA T 023618 (to G.H.) and the USPHS AR 22031 and NSF MCB-9630997 grants (to E.R.).

‡ UCLA.

§ Eötvös Lorand University.

[1] Abbreviations: ANP, 4-azido-2-nitrophenyl-putrescine; TG-ase, Ca^{2+}-independent bacterial transglutaminase; F-actin, filamentous (polymerized) actin; G-actin, monomeric actin; ANP-actin, ANP-labeled actin; S1, myosin subfragment-1; S1(A1), S1 containing light chain A1; S1(A2), S1 containing light chain A2; GS1, complex of G-actin and S1; G_2S1, complex of S1 with two G-actin molecules.

10.1021/bi9812874 CCC: $15.00
Published on Web 12/03/1998

OR). Bio-Rad protein assay was purchased from Bio-Rad laboratories (Hercules, CA). 4-azido-2-nitrophenyl-putrescine was synthesized as described by Hegyi et al. (*15*). Ca^{2+}-independent bacterial transglutaminase was a generous gift of Dr. K. Seguro, Ajimoto, Co., Inc. (Kawasaki, Japan).

Proteins. Rabbit actin and myosin were prepared from rabbit skeletal muscle according to the methods of Spudich and Watt (*17*) and Godfrey and Harrington (*18*), respectively. S1 from rabbit myosin was prepared following the procedures of Weeds and Pope (*19*). S1 isozymes, S1(A1) and S1(A2), were prepared as described by Chen and Reisler (*20*).

ANP Labeling and Cross-Linking of Actin. ANP labeling and photo-cross-linking of actin was carried out as described by Hegyi et al. (*15*) and Kim et al. (*16*).

Fractionation of ANP cross-Linked Actin Oligomers. Depolymerization of the cross-linked F-actin is the critical part of the fractionation procedure. Although extensive cross-linking of F-actin increases the relative fraction of cross-linked actin oligomers versus that of monomeric actin, at the same time it inhibits dramatically the depolymerization of F-actin. We found that the optimal balance was achieved when the extent of the cross-linking was between 40% and 60%. Such ANP−F-actin depolymerizes in G-buffer reasonably well and yields sufficient amounts of depolymerized cross-linked material. In a typical fractionation procedure 14 mg of ANP-labeled (44%) G-actin was mixed with 18 mg of unlabeled G-actin, polymerized by 2.0 mM $MgCl_2$, and cross-linked as described in the companion paper (*16*). Next, the cross-linked F-actin was depolymerized by dialysis against G-actin buffer for 2 days at 4 °C (with four buffer changes). The depolymerized actin was then sonicated twice for 30 s in the Branson bath sonicator B-220 (Branson for Co., Shelton, CT) and centrifuged at 40 000 rpm for 2 h, at 4 °C, to remove the remaining F-actin. The mixture of cross-linked actin oligomers obtained in this way (about 9.0 mg) was applied in a total volume of 3.0 mL to a Sephadex G-150 column (2.5 × 120 cm) equilibrated with G-actin buffer and chromatographed at an elution rate of 12.5 mL/h. The eluate was collected in 4.0 mL fractions. The entire cross-linking and fractionation procedure takes 6 days. To prevent bacterial growth, we supplemented the G-actin buffer (4.0 mM Tris-HCl, pH 7.6, 0.5 mM β-mercaptoethanol, 0.2 mM $CaCl_2$, and 0.2 mM ATP) with 0.02% NaN_3.

Analytical Ultracentrifugation. Sedimentation velocity experiments were carried out at 4 °C in a Beckman Model E analytical ultracentrifuge equipped with a photoelectric scanning system. Data collected into IBM PC files were transferred to a VAX 11/780 computer for analysis. The sedimentation of actin was monitored at 232 nm. Actin samples (4.0 μM) were examined in G-actin buffer (4.0 mM Tris-HCl, pH 7.6, 0.2mM $CaCl_2$, 0.2 mM ATP, and 0.5 mM β-mercaptoethanol) at a rotor speed of 56 000 rpm.

Pyrene Labeling of Actin. Actin was labeled at Cys 374 with *N*-(l-pyrenyl)iodoacetamide following the method of Cooper et al. (*21*). The extent of actin labeling was measured by using a molar extinction coefficient of $E_{344} = 2.2 \times 10^4$ M^{-1} cm^{-1} for the protein−dye complex (*22*).

Light-Scattering and Fluorescence Measurements. Both assays were carried out in a Spex Fluorolog spectrofluorometer (Spex Industries, Inc., Edison, NJ) at 25 °C in 250 μL cuvettes. Light scattering from actin solutions was monitored with excitation and emission monochromators set at 350 nm. For pyrene fluorescence measurements the excitation and emission wavelengths were 365 and 405, respectively. Protein concentrations in polymerization assays were adjusted to yield convenient times of polymerization.

S1 Binding to Actin. Binding S1 to pyrenyl actin was measured at 25 °C in G-actin buffer free of ATP. Free ATP was removed from actin solutions immediately prior to the binding experiments by passing actin through Sephadex G-50 spin columns. The binding of S1 to G-actin was monitored as described by Valentin-Ranc et al. (*10*), via the increase in pyrene fluroescence of the labeled actin. These data were plotted in the form of fluorescence ratios, F_r, that is, the fluorescence of pyrenyl actin in the presence of S1 over that in its absence. The binding of S1 to ANP cross-linked actin was assessed in competition experiments involving S1 and equimolar mixtures of ANP cross-linked actin and pyrenyl G-actin. The amount of free S1 and S1 bound to pyrenyl actin in that mixture was calculated from the fluorescence ratios observed for S1 binding to pyrenyl actin and the cross-linked actin dimers in the mixture (eqs 2 and 4 in Appendix). The dissociation constants of S1 from the dimers were obtained by fitting the values of F_r to an equation expressing the total concentration of S1 in terms of its independent binding equilibria with pyrenyl actin and the strongly and weakly binding sites on the cross-linked dimers (eq 5 in Appendix).

ATPase Assays. Because of limited amounts of ANP cross-linked actin, S1 ATPases in the presence of cross-linked actin dimers, trimers, and oligomers were determined by light-scattering measurements of the time to the onset of actin polymerization by S1, that is, the time required to hydrolyze ATP. This method is based on the observation that S1 does not polymerize G-actin containing MgATP until ATP is hydrolyzed (*23*). The solutions contained 4.0 μM actin in 4.0 mM Tris-HCl, pH 7.6, 0.5 mM β-mercaptoethanol, and 0.4 mM MgATP. ATP hydrolysis time was determined after the addition of 4.0 μM S1 to these solutions. Calibration light-scattering measurements on solutions of 4.0 μM S1 and G-actin verified a linear dependence of the hydrolysis time (time to the onset of polymerization) on the concentration of MgATP (between 0 and 0.5 mM). In all cases actin concentrations were defined using the molecular weight of G-actin.

Electron Microscopy. Samples polymerized by $MgCl_2$ were diluted to 2.3 μM immediately before spreading with polymerizing buffer. A 10 μL drop of sample was applied to a 500 mesh carbon-coated copper grid made hydrophilic by glow discharge. After one minute, a wedge of filter paper (Whatman No. 4) was touched to the edge of the grid to remove most of the sample. A 10 μL drop of aqueous 1% uranyl acetate was then applied to the grid. After 6 s this drop was wicked off and replaced with a fresh drop of stain. This procedure was repeated and a fourth drop of stain left on the grid for 45 s. A filter paper wedge wetted with stain was the used to remove the final drop of stain. The samples were allowed to air-dry.

Actin samples polymerized by equimolar S1 (4.0 μM) were mounted for electron microscopy as described previously (*23*). In brief, a 500 mesh carbon-coated copper grid made hydrophobic by holding it over the mouth of a beaker of molten dental wax for 20−30 s was floated on successive drops of sample diluted to an actin concentration 2.3 μM

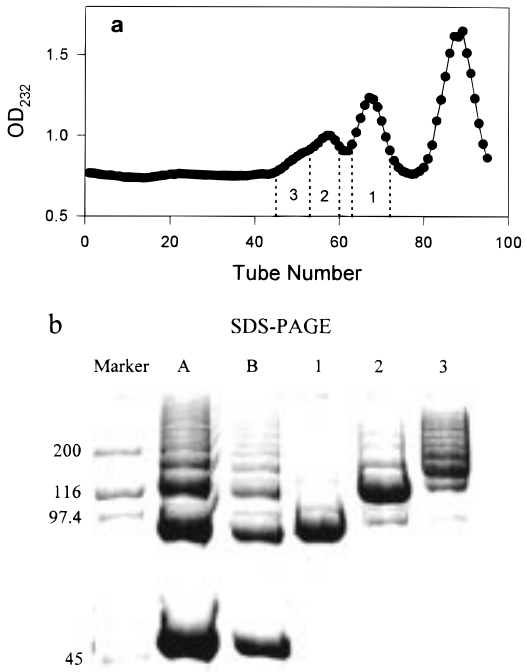

FIGURE 1: Fractionation of the ANP cross-linked actin dimers, trimers, and oligomers on a Sephadex G-150 column. (a) Protein elution profile from the Sephadex G-150 column. Depolymerized ANP cross-linked actin (9.0 mg) was applied to a Sephadex G-150 column equilibrated with G-buffer and eluted with the same buffer at a flow rate of 12 mL/h. Fractions (4.0 mL/fraction) marked by dotted lines were combined into three pools and concentrated on Amicon Centriprep −10 to between 0.5 and 0.9 mg/mL. (b) SDS−PAGE of ANP cross-linked actin species: lane A, ANP cross-linked F-actin; lane B, depolymerized ANP cross-linked actin applied to the Sephadex G-150 column; lane 1, fraction 1 containing ANP cross-linked actin dimers (1.50 mg); lane 2, fraction 2 containing ANP-actin trimers with minor contamination by dimers and oligomers (10%) (0.90 mg); lane 3, fraction 3 containing higher-order actin oligomers (0.14 mg). The total protein yield of each fraction is given in parentheses.

(60 s), 2 drops of buffer (6 s each), 2 drops of 10 mM sodium phosphate, pH 7.0 (6 s each), 4 drops of 1% aqueous uranyl acetate stain (6 s each), and a final drop of stain (45 s). The final stain droplet was removed by wicking with a filter paper wedge wetted with stain, and the samples were air-dried.

Samples were stored in a desiccator until they were examined in the electron microscope, usually on the next day. Grids were examined with a Hitachi H-7000 electron microscope operating at 75 kV with a condenser aperture of 200 μm and objective aperture of 50 μm. A liquid nitrogen cooled coldfinger (anti-contamination device) was used throughout. Micrographs were taken at an apparent microscope magnification of 30 000. Microscope magnification was calibrated using a diffraction grating replica (54 800 lines/in.).

Protein Assays. Protein concentrations of modified actin were determined by using the Bradford assay (*24*).

RESULTS

Fractionation of ANP Cross-Linked Actin Oligomers. Figure 1a (upper part) shows the elution profile of ANP cross-linked, depolymerized actin from the Sephadex G-150 column. The fractionation of actin was carried out as described in Materials and Methods. The eluted fractions were combined into three pools, as indicated in Figure 1, and concentrated on Centriprep-10 protein concentrators (Amicon Inc., Beverly, MA) to final protein concentrations between 0.5 and 0.9 mg/mL. Figure 1b (bottom part) shows SDS−PAGE profiles of ANP cross-linked actin prior to its depolymerization and fractionation (A), the mixture of oligomers applied to a Sephadex G-150 column (B), and the pooled fractions 1−3. As revealed by SDS−PAGE, fraction 1 contains cross-linked dimers and a minor amount of cross-linked trimers. Fraction 2 has about 90% of cross-linked trimers with a minor contamination by cross-linked dimers and higher-order oligomers. Fraction 3 contains cross-linked actin tetramers, higher-order oligomers, and a small amount of cross-linked trimers. Protein yields for each fraction are given in the legend to Figure 1.

To test whether the SDS−PAGE information indeed describes the size of the cross-linked species under nondenaturing solution conditions, we determined sedimentation coefficients for G-actin and the more homogeneous fractions 1 (dimers) and 2 (trimers). The sedimentation coefficients $s^\circ_{20,w}$ for G-actin and ANP cross-linked dimers and trimers were 3.52 ± 0.25, 5.55 ± 0.22, and 6.93 ± 0.12 S, respectively. These values, as well as sedimentation velocity boundaries monitored over the duration of the experiments, did not reveal any aggregation of the cross-linked actin. Notably, the sedimentation coefficient for the cross-linked dimer is similar to the value 5.0 ± 0.7 S obtained for actin dimers spontaneously formed in solution (*25*).

Binding of S1 to Cross-Linked Actin Dimers. In principle, the ANP cross-linked actin dimer should provide a stable material for assessing the proposed S1 binding to either two adjacent actins along the pitch helix in F-actin (*1*, *4*, *8*, *9*) or the longitudinal actin dimer, G_2, postulated by Valentin-Ranc & Carlier (*7*). Figure 2 shows the results of binding experiments on S1(A1) and S1(A2) and the ANP cross-linked actin dimers. The binding of S1 to cross-linked dimers was determined by monitoring the competition for S1 between equimolar concentrations of actin sites on dimers and on pyrenyl-G-actin. The inset to Figure 2 presents the titration of pyrenyl G-actin alone with S1(A1) and S1(A2) (i.e., the ratios of pyrene fluorescence for G actin in the presence of S1 to that for G-actin alone). The dissociation constants describing this binding are $K_p = 20 \pm 6$ and 30 ± 9 nM for S1A1 and S1A2, respectively. These values are consistent with previous results (*8*, *14*).

A remarkable feature of S1 binding to cross-linked dimers is the sharp biphasic shape of the S1 titration curve (Figure 2). The first part of this curve shows almost no fluorescence increase of pyrenyl G-actin (0.5 μM) by S1 isozymes in the presence of actin dimers (0.25 μM; i.e., 0.5 μM actin sites). This means that very little, if any, S1 binds to pyrenyl G-actin until actin dimers are occupied by one molecule of S1. Therefore, the affinity of S1 for such single occupancy of the dimer must be at least 10-fold stronger than that for the binding to pyrenyl G-actin. Examination of the second part of the titration curve, when the molar ratio of S1 to actin sites in dimers is between 0.5 and 1.0, suggests that the dimers and pyrenyl G-actin bind now S1 with similar affinities. In other words, the binding of a second S1 molecule to the dimer is much weaker than that of the first one. Accurate determinations of the dissociation constants, $K_{a,s}$ and $K_{a,w}$, for the strong and weak binding of the first and second S1 molecule to the actin dimer are complicated

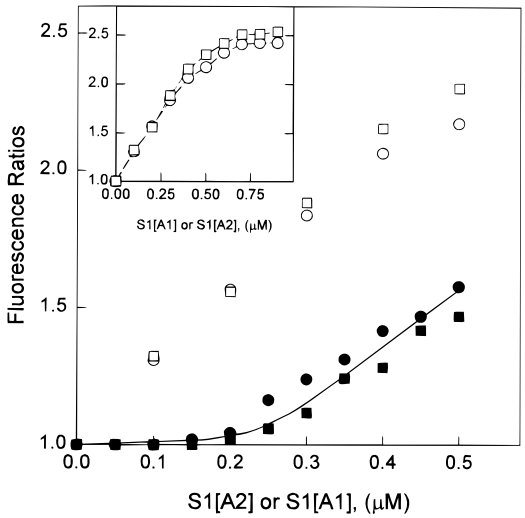

FIGURE 2: Binding of S1(A1) and S1(A2) to 0.5 μM pyrenyl G-actin and to the mixture of 0.5 μM pyrenyl G-actin and 0.25 μM ANP cross-linked actin dimers (i.e., 0.5 μM actin sites). The binding of S1 (A1) (□, ■) and S1(A2) (○, ●) to pyrenyl G-actin was monitored via changes in the ratios of pyrene fluorescence in the presence of S1 to that in its absence: ○, □, binding of S1 to 0.5 μM pyrenyl G-actin; ●, ■, binding of S1 to the mixture of 0.5 μM pyrenyl G-actin and 0.25 μM ANP cross-linked dimers. The solid curve represents the fit to the combined S1(A1) and S1(A2) data using eq 5 in the Appendix. The $K_{a,s}$ and $K_{a,w}$ values obtained by fitting the data to eq 5 were 0.2 ± 0.1 and 46 ± 25 nM, respectively. Inset: Complete set of fluorescence ratios for the binding of S1(A1) and S1(A2) to 0.5 μM pyrenyl G-actin obtained in the same experiment. The dashed curves were computed assuming one binding site for S1 on G-actin; $K_p = 20 \pm 6$ and 30 ± 9 nM for S1(A1) and S1(A2), respectively.

by the large difference between $K_{a,s}$ (for the dimer) and K_p (for pyrenyl G-actin). Estimates of $K_{a,s}$ and $K_{a,w}$ can be obtained by fitting the data in Figure 2 to an expression describing all forms of S1 present in the solution (eq 5 in Appendix). The best fit of the combined S1(A1) and S1(A2) data yields $K_{a,s}$ and $K_{a,w}$ values of 0.2 ± 0.1 nM and 46 ± 25 nM, respectively, (solid curve in Figure 2). Although the S1(A1) and S1(A2) data in Figure 2 can be fitted separately to eq 5 in the Appendix, the sensitivity of $K_{a,s}$ values to small changes in F_r at low S1 concentrations limits the value of such analysis. In line with this, simulation of the data with a range of selected $K_{a,s}$ values shows relatively small shifts of the calculated binding curve with up to 5-fold changes in $K_{a,s}$ (simulations not shown). Because of such inherent difficulties, the $K_{a,s}$ and $K_{a,w}$ values are viewed as estimates only, which demonstrate up to 100-fold stronger binding of the first than that of the second S1 to the dimer.

Activation of S1 MgATPase by ANP Cross-Linked Actin Oligomers. It is yet to be determined what constitutes the minimal functional unit of actin for the large activation of myosin ATPase by actin. Lheureux and Chaussepied et al. (*26*) suggested that the longitudinal actin dimer may be such a unit. This possibility was tested by assaying the ability of the cross-linked actin oligomers to activate S1 MgATPase. Because of limited amounts of the cross-linked material, we used light-scattering measurements instead of conventional colorimetric assays to monitor the rate of ATP hydrolysis by actin-S1 complexes. The reaction mixtures contained 4.0 μM G-actin or cross-linked actin in G-actin buffer with 0.4 mM MgATP. ATP hydrolysis was started with the addition of 4.0 μM S1 to these mixtures. When all of the ATP in the system was hydrolyzed, we observed an increase in light scattering corresponding to the onset of S1-induced polymerization of actin. Table 1 lists ATP hydrolysis rates by G-acto-S1 and cross-linked actin-S1 complexes per 1 μM of S1 per 1 s derived from such data. Without correction for intrinsic ATPase of S1 alone, the activation values are 2.6, 4.4, and 6.6 times for G-actin, cross-linked dimers, and cross-linked trimers and oligomers, respectively. These results show that single-stranded cross-linked oligomers of actin do not activate S1 ATPase in a manner similar to that of F-actin despite their strong rigor binding of S1. Either the minimal functional unit of F-actin must be double-stranded, or longer oligomers are required for S1 ATPase activation.

Table 1: MgATPase of S1 in the Presence of Actin

actin	ATPase (s^{-1})
G-actin	0.13
cross-linked dimers	0.22
cross-linked trimers	0.33
cross-linked oligomers	0.33
F-actin	3.5

[a] The rates of ATP hydrolysis by S1 in the presence of various actin species were determined at 23 °C by light scattering measurements of the time to the onset of actin (4.0 μM) polymerization by S1 (4.0 μM) in the presence of 0.4 mM MgATP. In the case of F-actin, 0.4 mM MgATP was added to the pre-formed F-actin-S1 (4.0 μM) and the clearance time (time of ATP hydrolysis) of this solution was determined by light-scattering measurements. MgATP turnover rate of S1 alone (0.05 s^{-1}) was determined by a calorimetric assay.

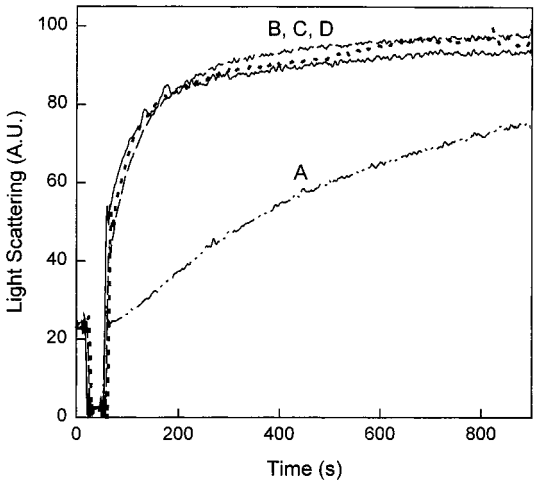

FIGURE 3: Light-scattering measurements of $MgCl_2$-induced polymerization of ANP cross-linked actin. The polymerization of actin (5.0 μM) was initiated by the addition of 2.0 mM $MgCl_2$ to actin: A, G-actin; B, ANP cross-linked actin dimers; C, ANP cross-linked actin trimers; D, ANP cross-linked oligomers.

Polymerization Properties of Single-Stranded Cross-Linked Actin Oligomers. *$MgCl_2$-Induced Polymerization.* Figure 3 shows light-scattering measurements of $MgCl_2$-induced polymerization of cross-linked actin oligomers and G-actin. Within the resolution of these experiments, all cross-linked materials polymerize at a similar rate, much faster than that of G-actin. When small amounts of cross-linked actin are added to G-actin, the acceleration of polymerization by $MgCl_2$ is increased with the size of the cross-linked species (data not shown). Noticeable in these data is the absence of nucleation step in the polymerization of cross-linked actin. This means that the cross-linked longitudinal actin dimers, trimers, and oligomers are able both to nucleate

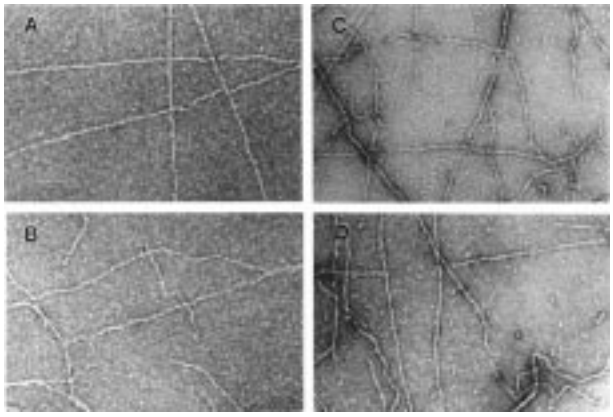

FIGURE 4: Electron micrographs of actin filaments: A, un-cross-linked F-actin; B, filaments re-assembled from ANP cross-linked actin dimers; C, filaments re-assembled from ANP cross-linked actin trimers; D, filaments re-assembled from ANP cross-linked actin oligomers. All filaments were obtained by polymerization of actin with 2.0 mM $MgCl_2$. The bar corresponds to 1000 Å.

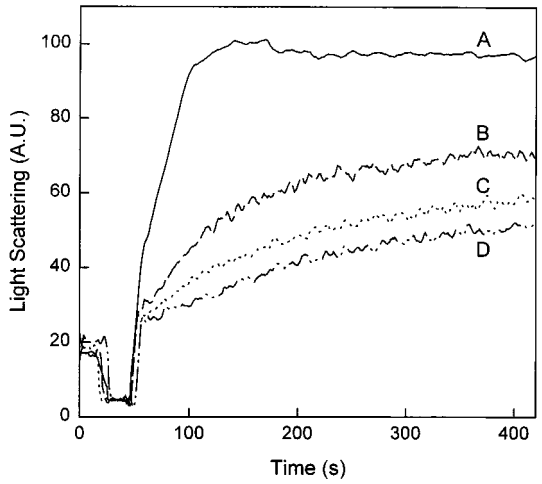

FIGURE 5: Light-scattering measurements of S1-induced polymerization of ANP cross-linked actin. The polymerization of actin (5.0 μM) in G-actin buffer was initiated by the addition of S1 (5.0 μM). Individual light-scattering traces correspond to the following: A, G-actin; B, ANP cross-linked actin dimers; C, ANP cross-linked actin trimers; D, ANP cross-linked oligomers.

$MgCl_2$-induced filament formation and to elongate the growing filaments. Electron micrographs of F-actin assembled from G-actin, cross-linked actin dimers, trimers, and oligomers do not reveal any major structural differences among these filaments except for the tendency to show occasional bending and shorter length, especially for those made from cross-linked oligomers (Figure 4).

S1-Induced Polymerization. One of the characteristic properties of acto-S1 interactions is the ability of S1 to polymerize G-actin into F-actin filaments. Results presented in this and the companion paper (*16*) reveal that the ANP cross-linked actin dimers and oligomers polymerize to form functional filaments (*16*) and that they bind S1 isozymes. Figure 5 shows the polymerization of G-actin and cross-linked actin oligomers by S1 as monitored by light-scattering measurements. Surprisingly, in contrast to the $MgCl_2$-induced polymerization, cross-linked actin dimers, trimers, and oligomers are polymerized by S1 less well than G-actin. The rates of polymerization by S1 and final light-scattering plateau values for mixtures of S1 with actin dimers, trimers, and oligomers decrease in that order. The cross-linked actin

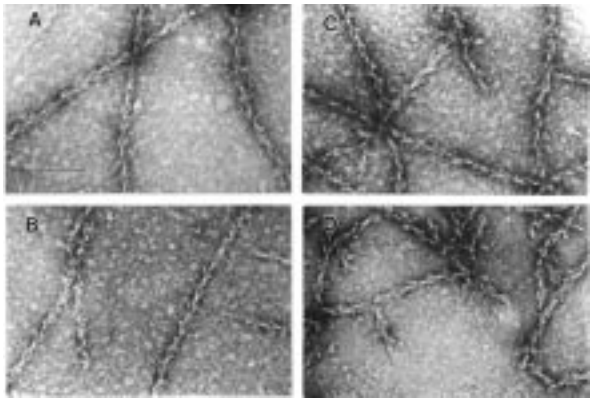

FIGURE 6: Electron micrographs of actin polymerized by S1: A, un-cross-linked actin polymerized by S1; B, cross-linked dimers polymerized by S1; C, cross-linked trimers polymerized by S1; D, cross-linked oligomers polymerized by S1. The bar corresponds to 1000 Å.

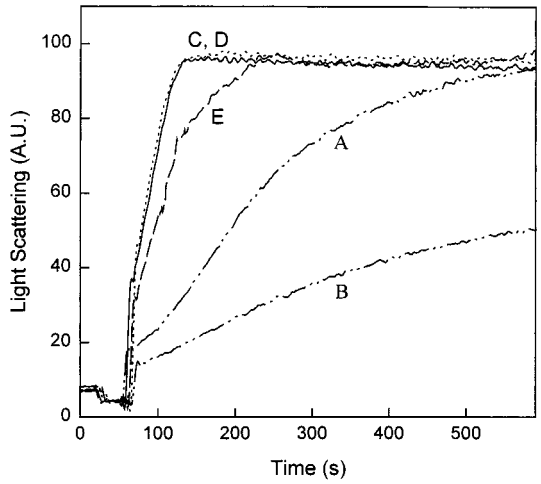

FIGURE 7: Nucleation of S1-induced polymerization of G-actin by ANP cross-linked actin dimers. The polymerization of actin (2.5 μM G-actin) was initiated by the addition of S1 (2.5 μM). The polymerization reaction was followed as a function of time by measuring the light scattering at 350 nm. Individual traces correspond to A, G-actin; B, ANP cross-linked actin dimers; C, 96% G-actin + 4% ANP cross-linked actin dimers; D, 80% G-actin + 20% ANP cross-linked actin dimers; E, 50% G-actin + 50% ANP cross-linked actin dimers.

polymerized by S1 was also examined by electron microscopy (Figure 6). The observed actin-S1 complexes formed arrowheaded structures, which were shorter than those obtained with S1 and un-cross-linked G-actin. This was most striking for S1-polymerized oligomers, for which few long arrowhead structures could be detected. These short arrowhead structures explain the reduced light scattering of the cross-linked actin sample (Figure 5) and show that the complexes of cross-linked actin with S1 are not the optimal structural units for filament assembly.

To test which step of actin polymerization by S1, the nucleation or elongation, is inhibited by ANP cross-linking reactions, we examined the assembly of cross-linked dimers in greater detail. According to our binding results (Figure 2), such dimers should bind preferentially one molecule of S1 to yield ternary complexes presumably corresponding to the proposed G_2S1 assembly intermediates (*8*). Figure 7 shows the polymerization by S1 of mixtures of G-actin and cross-linked dimers at different G-actin−actin dimer ratios.

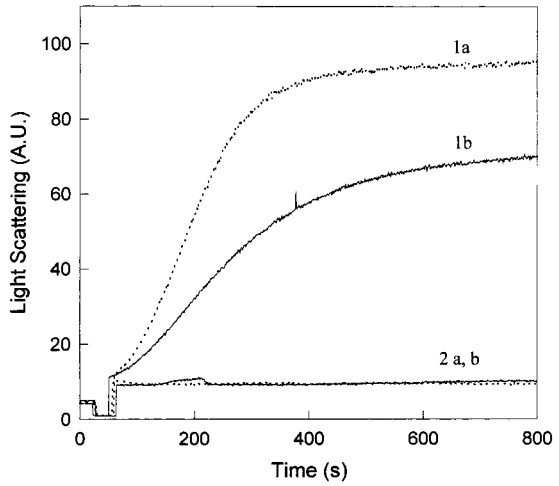

FIGURE 8: Light-scattering measurements of actin polymerization induced by S1(A1) and S1(A2). The polymerization of 2.0 μM actin in G-actin buffer was initiated by the addition of 2.0 μM S1(A1) (curves 1a,b) or S1(A2) (curves 2a,b). Dotted curves (1a, 2a) represent the polymerization of G-actin, and solid curves (1b, 2b) describe the polymerization of the cross-linked actin dimer.

Interestingly, low concentrations of cross-linked dimers (4%, and possibly even less) accelerate strongly the polymerization of G-actin by S1. High concentrations of the dimer, 50% and above, inhibit actin polymerization by S1. Thus, the cross-linked dimers accelerate the nucleation step in the polymerization of G-actin by S1 or provide such nuclei if the formation of G_2S1 is indeed an essential assembly step. The inhibition of S1-induced actin assembly for cross-linked dimers alone (curve B in Figure 7) suggests that the elongation of actin filaments is impaired when G_2S1 or $G_2(S1)_2$ units must be used in this step of the assembly reaction. When dimer S1 was the dominant complex present in the solution, that is, when the polymerization of actin by S1 was monitored at 2:1 molar ratios of these proteins, rather than at the equimolar concentrations used in experiments shown in Figures 5 and 7, the relative inhibition of actin assembly by S1 due to the cross-linked dimers was increased by 50%. Thus, at concentrations of actin and S1 set at 5.0 μM (Figure 5) the half time ($t_{1/2}$) for actin polymerization by S1 was 2-fold longer with the cross-linked dimers (74 s) than with the un-cross-linked G-actin (36 s). The $t_{1/2}$ value was 3-fold longer for the dimers (290 s) than for G-actin (90 s) when actin and S1 concentrations were 5.0 and 2.5 μM, respectively (data not shown). This comparison confirms the suggestion that G_2S1 impairs the elongation of actin filaments relative to S1 complexes with G-actin.

A significant feature of actin polymerization by S1 is the large difference in the rate of this reaction depending on the isoform of S1, S1(A1) or S1(A2), which binds to G-actin. The much faster polymerization of actin by S1(A1) than by S1(A2) (*10*, *14*, *20*, *27*) has been attributed to the binding of light chain A1 to a second actin molecule in the vicinity of its C-terminus. Such a binding would stabilize the G_2S1 and facilitate actin polymerization. Alternatively, it is possible that the main contribution of the 41 N-terminal residues of A1 to actin polymerization is via structural changes in the actin dimer induced by A1 binding to the C-terminus region (*14*). The cross-linked dimers provide additional information on this issue. As shown in Figure 8, the polymerization of actin by S1(A1), in analogy to that by the unfractionated S1 (Figure 5), proceeds at a slower rate with the cross-linked dimers than the un-cross-linked G-actin (Figure 8, curves 1a and 1b). More notable is the fact that the polymerization of actin by S1(A2) is not accelerated by the dimers (Figure 8, curves 2a and 2b). This result shows that the presence of stable dimers, which can nucleate actin polymerization by S1 (curves C and D in Figure 7), is insufficient for bridging the kinetic gap between the polymerization of actin by S1(A1) and S1(A2).

DISCUSSION

This paper describes the purification and properties of isolated actin oligomers cross-linked by ANP between Gln-41 and Cys-374 on two adjacent monomers of the same strand in the long-pitch helix in F-actin. ANP cross-linked F-actin, which is the source of the purified actin oligomers, depolymerizes more readily than the pPDM cross-linked F-actin (our unpublished results and ref *28*) and enables the isolation of cross-linked longitudinal dimers, trimers, and higher oligomers. The identity of these dimers and trimers and their low tendency, if any, to aggregate spontaneously in G-actin buffer to higher-order species has been confirmed in sedimentation velocity experiments. In contrast to these ANP cross-linked species, trimers and oligomers could not be obtained through the depolymerization of pPDM cross-linked F-actin (*28*). Because pPDM, unlike ANP, cross-links adjacent actin monomers on two opposing strands of F-actin (*29*), the above differences point to the importance of lateral bonds between the two strands in the stabilization of the actin filament structure.

Isolated ANP cross-linked actin dimers were found to bind two S1 molecules per actin dimer. Because differences between S1(A1) and S1(A2) titrations in Figure 2 are small, and large differences between K_p and $K_{a,s}$ values prelude accurate determinations of $K_{a,s}$ and $K_{a,w}$, all S1 binding data are fitted to a single curve (Figure 2). The binding of the first S1 to dimers is about 100-fold stronger than that to pyrenyl G-actin, while the affinity of the second S1 for dimers is about the same as its affinity for pyrenyl G-actin. This is true for both S1(A1) and S1(A2) isozymes of S1 (when the data are fitted to separate curves for each isozyme the corresponding $K_{a,s}$ and $K_{a,w}$ values are 0.1 and 21 nM for S1(A1), respectively, and 0.2 and 85 nM for S1(A2); curves not shown), indicating that the differences between 1:1 and 1:2 S1 binding to actin are not related to the light chain composition of S1. These observations are consistent with the molecular model of F-actin-S1 structure (*1*, *30*) and the results of cross-linking of F-actin-S1 complexes (*4*). According to both studies S1 binds to two adjacent actin monomers along one strand of the long-pitch helix of the actin filament. On the basis of the F-actin-S1 model we assume that both actin monomers in the dimer contribute to the binding of the first S1; therefore, the binding is strong. It may be noted that the value of $K_{a,s}$ suggests that this binding is more than 10-fold stronger than that indicated by kinetic measurements of S1 binding to F-actin [$K_d = 5$ nM; ref *35*]. The interpretation of this difference must await more sensitive and accurate measurements of $K_{a,s}$. The second S1 binds only to one of the monomers in the actin, and thus, the binding affinity for this interaction is much smaller. A decrease in the affinity of the second S1 for the dimer is consistent with the observed negative cooperativity of S1

binding to F-actin (*35*). Overall, if it is assumed that the cross-linked dimer is similar to spontaneously formed actin dimers, then our binding results support the view on the existence of G_2S1 complexes (*8*). According to these authors, the G_2S1 complex is an important intermediate in the S1-induced actin polymerization.

Interestingly, despite the strong rigor binding of S1, the unpolymerized cross-linked dimers, trimers, and higher oligomers activate very little the MgATPase of S1. However, the same cross-linked actin species activate the S1 ATPase after polymerization into filaments (*16*) indicating that the weak activation by the unpolymerized cross-linked actin is not a consequence of the cross-linking. These results imply that the binding of S1 to two actin monomers aligned on the long-pitch helix may be necessary (*26*) but is not a sufficient condition for the activation of myosin ATPase. As in the case of G-actin (*31*), the small activation of myosin ATPase activity by unpolymerized oligomers might be caused by their low affinity for S1−nucleotide complexes. It is also possible that the low activation of S1 ATPase by oligomers is due to the lack of proper structural arrangement of actins, which is necessary for the activation and may or may not be needed for the weak binding of S1 to actin. It is possible that only double-stranded actin oligomers can fully activate the myosin ATPase. Lateral bonds, which connect the two strands and may allosterically affect the actin−myosin interface, appear to be needed for actin activation. The possibility that lateral bonds between actin subunits in F-actin might modify the F-actin-S1 interface is indicated also by S1-induced perturbation of the pyrene probe attached to hydrophobic loop 262−274 in mutant yeast actin (*32*). According to models of F-actin structure (*33*, *34*) this loop stabilizes interstrand interactions in actin filaments.

The $MgCl_2$-induced polymerizations of ANP cross-linked dimers, trimers, and oligomers proceed at similar rates, which are much faster than that of G-actin. Since, according to analytical ultracentrifugation, these species are not aggregated in solution, all of them, including the cross-linked dimers, can serve as efficient nuclei in the polymerization process. The filaments formed from cross-linked dimers, trimers, and oligomers by $MgCl_2$ are structurally and functionally competent (*16*).

In contrast to the above, S1-induced polymerization of cross-linked oligomers is different from that of normal G-actin. Mostly short, S1-decorated filaments are produced from cross-linked oligomers by S1, while long decorated filaments are obtained from intact, un-cross-linked actin. Moreover, the rate of polymerization of undiluted cross-linked dimers, trimers, and oligomers is much slower than that of G-actin. On the other hand, even small amounts of cross-linked dimers can act as efficient nucleating agents in the S1-induced polymerization of G-actin. This finding is consistent with, but does not prove, the proposed role of G_2S1 complexes in the S1-induced polymerization of G-actin (*8*) (assuming that the structure of the dimer−S1 complex is similar to that of G_2S1). Since the nucleation phase of G-actin polymerization by S1 is not inhibited by the cross-linking, the overall slow polymerization rate and the shorter filaments imply that the complexes of S1 with ANP cross-linked dimers and higher-order oligomers do not support well the elongation phase of the polymerization process. These results indicate that the G_2S1 and, to a smaller extent, $G_2(S1)_2$ units are not the kinetically favored intermediates of filament elongation. It is possible to rationalize such results by assuming that the actin−S1 complexes must undergo some changes to establish lateral bonding interactions and for their incorporation into filaments. These changes may be inhibited in the cross-linked dimers, because of their reduced structural flexibility, to a greater extent than in the spontaneously formed G_2S1 or $G_2(S1)_2$ units. It has been suggested before that the formation of lateral bonds between F-actin subunits is energetically unfavored and is the limiting step in the nucleation of actin assembly (*8*). Our results indicate the importance of these bonds for filament growth. Moreover, because cross-linked actin dimers do not activate myosin ATPase well and are polymerized less well by S1 than G-actin, our results suggest also that G_2S1 or $G_2(S1)_2$ complexes do not provide a faithful model of the F-actin-S1 interface. This, of course, assumes that the complexes of S1 and the cross-linked dimers are similar to G_2S1 and $G_2(S1)_2$. The differences between actin interfaces in F-actin-S1 and G-actin-S1 complexes were reviewed by Lheureux and Chaussepied (*31*).

Changes in actin structure appear to be involved also in the initial stages of its polymerization by S1. Because the dimers do not abolish the kinetic difference between S1(A1)- and S1(A2)-induced assembly of actin, the kinetic advantage of S1(A1) must be due to factors other than dimer stabilization via A1 binding to a second actin molecule.

In conclusion, we found that unaggregated oligomers can be isolated from ANP cross-linked F-actin. The oligomers aligned along the long pitch of F-actin bind S1 strongly but do not activate the S1 ATPase much. The oligomers polymerize into normal length functional filaments upon the addition of $MgCl_2$, and even the smallest oligomer, the dimer, serves as an efficient nucleating agent. The oligomers also polymerize upon the addition of S1, but this polymerization is slow and results in short filaments because of retardation of the elongation process. Additional functional and structural characterization of the purified oligomers should contribute to a better understanding of actin polymerization and filament structure.

APPENDIX

When f is assigned to the molar fluorescence of free pyrenyl actin and Nf is assigned to that of pyrenyl actin bound to S1, the total fluorescence of a pyrenyl actin and S1 solution is represented by

$$F = [\mathrm{sp}]Nf + [\mathrm{p}]f$$

Where [sp] and [p] are the concentrations of S1-bound and free pyrenyl actin. The fuorescence ratio, F_r, for this solution is defined as

$$F_r = \frac{F}{F_o} = \frac{[\mathrm{sp}]Nf + [\mathrm{p}]f}{[\mathrm{p_o}]f} \qquad (1)$$

Where $[p_o]$ is the total concentration of pyrenyl actin and F_o is the fluorescence of pyrenyl actin in the absence of S1. Substitution of $[p] = [p_o] - [sp]$ and simple transformations lead to eq 2, which expresses the concentration of pyrenyl actin bound to S1 in terms of fluorescence ratios.

$$[sp] = (F_r - 1)\frac{[p_o]}{N - 1} \quad (2)$$

The value of N is obtained from eq 1 when the binding of pyrenyl actin is saturated by S1, that is, when $[p] \approx O$ and $[p_o] \approx [sp]$. According to data shown in the inset to Figure 2, $N = 2.5$.

The total concentration of S1, $[s_o]$, in the presence of pyrenyl actin and cross-linked actin dimers is given by

$$[s_o] = [s] + [sp] + [sa_s] + [sa_w] \quad (3)$$

Where $[s]$ is the concentration of free S1, and $[sa_s]$ and $[sa_w]$ are the concentrations of S1 bound strongly and weakly to the dimer, respectively. Two different affinities of S1 for actin in the dimer were deduced from qualitative examination of the binding data shown in Figure 2. To simplify data analysis it is assumed arbitrarily that the strong and weak binding of S1 to the dimer can be described by independent equilibria. The concentrations of s, sa_s, and sa_w in eq 3 are obtained from the mass action laws:

$$K_p = \frac{[s][p]}{[sp]}; \quad K_{a,s} = \frac{[s][a_s]}{[sa_s]}; \quad K_{a,w} = \frac{[s][a_w]}{[sa_w]}$$

Where K_p, $K_{a,s}$, and $K_{a,w}$ are the dissociation constants describing the binding of S1 to pyrenyl actin, and the strong and weak binding of S1 to the dimer, respectively. $[a_s]$ and $[a_w]$ are the concentrations of free strongly and weakly binding actins in the dimer pool. With definition of K_p and eq 2, the concentration of free S1 is given by

$$[s] = \frac{K_p(F_r - 1)}{N - F_r} \quad (4)$$

After substituting the expressions for $[s]$, $[sp]$, $[sa_s]$, and $[sa_w]$ into eq 3 and some simple algebraic manipulations, the final expression for $[s_o]$ assumes the form

$$[s_o] = \frac{K_p}{\alpha} + \frac{[p_o](N - F_r)}{\alpha(N - 1)} + \frac{[a_{s,o}]K_p}{K_p + \alpha K_{a,s}} + \frac{[a_{w,o}]K_p}{K_p + \alpha K_{a,w}} \quad (5)$$

where $\alpha = (N - F_r)/(F_r - 1)$ and $[a_{s,o}] = [a_{w,o}]$ are the total concentrations of strongly and weakly binding sites for S1 on the dimer, which are also equal to the total concentration of the cross-linked dimer.

The two unknown in eq 5 are the dissociation constants $K_{a,s}$ and $K_{a,w}$ for the strong and weak binding of S1 to the dimer. K_p is known from measurements of S1 binding to pyrenyl actin (inset to Figure 2). The values of $K_{a,s}$ and $K_{a,w}$ are solved by fitting the experimental data of F_r to eq 5. The calculated curve (using Sigma 4) in Figure 2 represents the best fit of all S1 data using the following parameters: $K_p = 0.02\ \mu M$, $[p_o] = 0.5\ \mu M$, $[a_{s,o}] = 0.25\ \mu M$, $[a_{w,o}] = 0.25\ \mu M$, and $N = 2.5$.

REFERENCES

1. Rayment, I., Holden, H. M., Whittaker, M., Yohn, C. B., Lorenz, M., Holmes, K. C., and Milligan, R. A. (1993) *Science 261*, 58−65.
2. Schroeder, R. R., Manstein, D. J., Jahn, W., Holden, H., Rayment, I., Holmes, K. C., and Spudich, J. A. (1993) *Nature 364*, 171−174.
3. Milligan, R. A. (1996) *Proc. Natl. Acad. Sci. U.S.A. 93*, 21−26.
4. Andreev, O. A., Andreeva, A. L., Markin, V. S., and Borejdo, J. (1993) *Biochemistry 32*, 12046−12053.
5. Bonafe, N., and Chaussepied, P. (1995) *Biophys. J. 68*, S35−S43.
6. Arata, T. (1996) *Biochemistry 35*, 16061−16068.
7. Valentin-Ranc, C., and Carlier, M. F. (1992) *J. Biol. Chem. 267*, 21543−21550.
8. Fievez, S., Pantaloni, D., and Carlier, M.-F. (1997) *Biochemistry 36*, 11837−11842.
9. Fievez, S., Carlier, M. F., and Pantaloni, D. (1997) *Biochemistry 36*, 11843−11850.
10. Valentin-Ranc, C., Combeau, C., Carlier, M. F., and Pantaloni, D. (1991) *J. Biol. Chem. 266*, 17872−17879.
11. Carlier, M.-F., Didry, D., Erk, I., Lepault, J., and Pantaloni, D. (1994) *J. Biol. Chem. 269*, 3829−3837.
12. Blanchoin, L., Fievez, S., Travers, F., Carlier, M.-F., and Pantaloni, D. (1995) *J. Biol. Chem. 270*, 7125−7133.
13. Kasprzak, A. A. (1994) *Biochemistry 33*, 12456−12462.
14. Lheureux, K., Forne, T., and Chaussepied, P. (1993) *Biochemistry 32*, 10005−10014.
15. Hegyi, G., Mak, M., Kim, E., Elzinga, M., Muhlrad, A., and Reisler, E. (1998) *Biochemistry 37*, 17784−17792.
16. Kim, E., Bobkova, E., Miller, C. J., Orlova, A., Hegyi, G., Egelman, E. H., Muhlrad, A., and Reisler, E. (1998) *Biochemistry 37*, 17801−17809.
17. Spudich, J., and Watt, S. (1971) *J. Biol. Chem. 246*, 4866−4871.
18. Godfrey, J. E., and Harrington, W. F. (1970) *Biochemistry 9*, 886−893.
19. Weeds, A., and Pope, N. (1977) *J. Mol. Biol. 111*, 129−157.
20. Chen, T., and Reisler, E. (1991) *Biochemistry 30*, 4546−4552.
21. Cooper, J. A., Walker, S. B., and Polard, T. D. (1983) *J. Muscle Res. Cell Motil. 4*, 253−262.
22. Kouyama, T., and Mihashi, K. (1981) *Eur. J. Biochem. 114*, 33−38.
23. Miller, L., Phillips, M., and Reisler, E. (1988) *J. Biol. Chem. 263*, 1966−2002.
24. Bradford, M. M. (1976) *Anal. Biochem. 72*, 248−254.
25. Attri, A. K., Lewis, M. S., and Korn, E. D. (1991) *J. Biol. Chem. 266*, 6815−6824.
26. Lheureux, K., and Chaussepied, P. (1995) *Biochemistry 34*, 11445−11452.
27. Chaussepied, P., and Kasprzak, A. A. (1989) *Nature 342*, 950−953.
28. Mockrin, S. C., and Korn, E. D. (1981) *J. Biol. Chem. 256*, 8228−8233.
29. Elzinga, M., and Phelan, J. J. (1984) *Proc. Natl. Acad. Sci. U.S.A. 81*, 6599−6602.
30. Rayment, I., and Holden, H. M. (1993) *Curr. Opin. Struct. Biol. 3*, 944−952.
31. Lheureux, K., and Chaussepied, P. (1995) *Biochemistry 34*, 11435−11444.
32. Feng, L., Kim, E., Lee, W.-L., Miller, C. J., Kuang, B., Reisler, E., and Rubenstein, P. A. (1997) *J. Biol. Chem. 272*, 16829−16837.
33. Holmes, K. C., Popp, D., Gebhard, D., and Kabsch, W. (1990) *Nature 347*, 44−49.
34. Lorenz, M., Popp, D., and Holmes, K. C. (1993) *J. Mol. Biol. 234*, 826−836.
35. Blanchoin, L., Didry, D., Carlier, M.-F., and Pantaloni, D. (1996) *J. Biol. Chem. 271*, 12380−12386.

BI9812874